FUDMA Journal of Sciences (FJS)
ISSN online: 2616-1370
ISSN print: 2645 - 2944
Vol. 3 No. 4, December, 2019, pp 15 -19

SIMULATION-BASED IMPLEMENTATION OF MAGNETIC FIELD ORIENTATION FOR ACCURATE INDUCTION

***[1]Okpala, C. N. and [2]Lawan, S. M.**

[1]Department of Physics, Federal University Dutsin - Ma, Katsina State, Nigeria
[2]Department of Electrical Engineering, Kano University of Science and Technology, Wudil Kano State

*Corresponding Authors email: cokpala@fudutsinma.edu.ng

ABSTRACT

The traditional methods for printed circuit boards (PCB) diagnoses is still incapable of achieving the desired speed and accuracy. These methods require a direct connection to PCB traces and pads to perform the checkups, which takes a lot of time maybe up to hours or days to discover the fault. In this paper, a new design for a mini coil which induces electric current in a narrow copper trace inside the PCB is presented. The new mini coil features the ability to stimulate electromotive force in a narrow path (0.8-1.2) mm avoiding any considerable effect on the surrounding copper traces. The design of the new mini coil was carried out by Finite Element Method Magnetics simulation software. This paper shows the magnitude of flux density β along a parallel PCB. The design of this mini coil represents the first part of a whole model design for PCB diagnosis.

Keywords*:* printed circuit board, PCB, magnetic, induction, coil, copper, traces

INTRODUCTION

Electromagnetic induction (MI) is a magnetic stimulation that generates an electric current by producing a potential difference (voltage) across a conductor under a varying magnetic field (Martin, 2011). This method is used widely for motors, transformers, generators and other purposes. However, despite the rise in popularity of using magnetic fields, its usage in electronic boards diagnosing is still limited. MI has been shown to create a variety of electromotive forces depending on the field intensity, frequency, conductor resistivity, permittivity and conductivity. Moreover, the properties of magnetic coil affect greatly the response to MI. Each coil has its own shape, size and configuration. Independent of coils properties, most of the coils are designed for transformer applications and their sizes are customized for this purpose (Hadass *et al, 2011*). A number of structures exist inside a printed circuit board (PCB) that can be used to form transmission lines. Traces are used to route time-varying currents around on PCBs (Gisin and Pantic-Tanner, 2001). The exposure of copper traces inside PCB to magnetic field will stimulate electrons to move constituting what is called electromotive field.

Models for estimating radiated emissions due to electric field coupling have been discussed in (Shim and Hubing, 2005). A magnetic field coupling model was presented in (Hockanson *et al.* 1997), and equations were developed to calculate this coupling for microstrip trace geometries.

Shaowei *et al* (2008) demonstrated how magnetic field coupling measurements made with a Transverse Electromagnetic (TEM) cell can be used to determine a magnetic moment that can be used to quantify the ability of the board to drive common-mode current on attached cables due to magnetic field coupling. A suitable numerical simulation method for the coupling of an external electromagnetic field to PCB traces was presented by (Marco, 2005). It is based on the method of moments (MoM), applied to an equivalent-wire model for the traces, and allows the coupled voltages and currents to be determined at any point on the structure for an arbitrary external plane-wave field.

According to Gisin and Pantic-Tanner (2001), one way to reduce radiation along PCB edges is to add two outer ground plane layers that are shorted along the periphery either with closely spaced traces or by plating the edges of the printed circuit board. Both of these reduce edge emissions significantly. However, the reflections from the shorted edges reflect back into the PCB, increasing the magnitude of internal resonant peaks and secondary coupling back onto the traces. The coupling can be significant enough to create signal integrity problems such as ground bounce and simultaneous switching output (SSO) noise.

Many previous studies analyzed the noise caused by a magnetic field on circuits. This noise relates to Faraday's law which states "The induced electromotive force in any closed circuit is equal to the negative of the time rate of change of the magnetic flux through the circuit" (Young and Freedman, 1998). Different methods have been proposed and implemented by researchers, but dealing with narrow width remains a great task that needs to be filled. Copper traces characterized by its narrow width is around 10 mil and traces normally are so convergent to each other. The main challenge is to stimulate the EMF on a single trace avoiding any considerable stimulation for the surrounding traces.

METHODOLOGY

The design of the coil was carried out using finite element solver for 2D and axisymmetric magnetic software. Pure iron was used as the core since it has a high relative permittivity μ_x=14782 and acceptable electrical conductivity σ = 10.44 M s/m. The core was laminated in a plane, with each laminate having a thickness of 0.42 mm and a lamination fill factor equal to 1. The windings consist of 1000 turns of insulated copper wire 36 AWD, which has a diameter 0.127 mm, electrical conductivity σ =58 Ms/m and a magnetic permittivity = 1. The standard coils shown in figure.1 create a magnetic field with a wide band. That means the electromotive force (EMF) will arise in a wide band.

According to Fraday's law of induction, each turn will cause independent magnetic field. Hence, a uniform field yields opposite to the windings (John and Stanislaw, 2003). This field will be uniform and equilibrium as long as the axis faces the windings as shown in figure 2a.

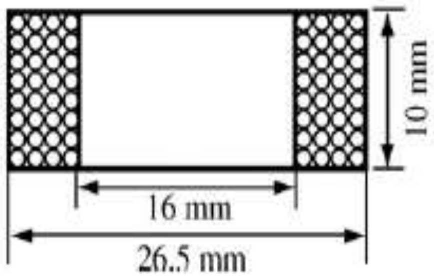

Fig.1: Standard coil with inner diameter 16mm and outer diameter 26.5mm and a length 10mm

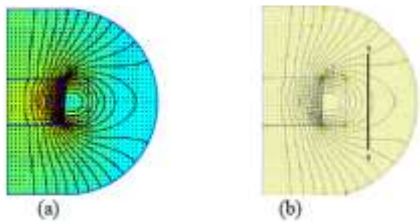

Fig. 2: The right windings of a coil and a resultant uniform magnetic field opposite to it.
b- XY contour opposite to the right windings considered to calculate B.

To know the distribution of magnetic intensity, a finite element solver was used, a contour x-y with length 20 mm and 5 mm away from the right edge of winding. In this case, the field intensity (H) and flux density (B) must obey:

$$xH = J \quad (1)$$

$$B = 0 \quad (2)$$

Subject to a constitutive relationship between B and H for each material:

$$B = \mu H \quad (3)$$

where μ is the magnetic relative permittivity of the media. If a material is nonlinear (for example, saturating iron or alnico magnets), the permeability, μ is actually a function of B:

$$\mu = \frac{B}{H}(B) \quad (4)$$

FEMM goes about finding a field that satisfies (1)-(3) via a magnetic vector potential approach. The flux density is written in terms of the vector potential, A, as:

$$B = xA \quad (5)$$

Now, this definition of B always satisfies (2). Then, (1) can be rewritten as:

$$x[1/\mu(B)]xA = J \quad (6)$$

RESULTS

The chart which shows the magnetic intensity for the x-y contour is shown in figure 3:

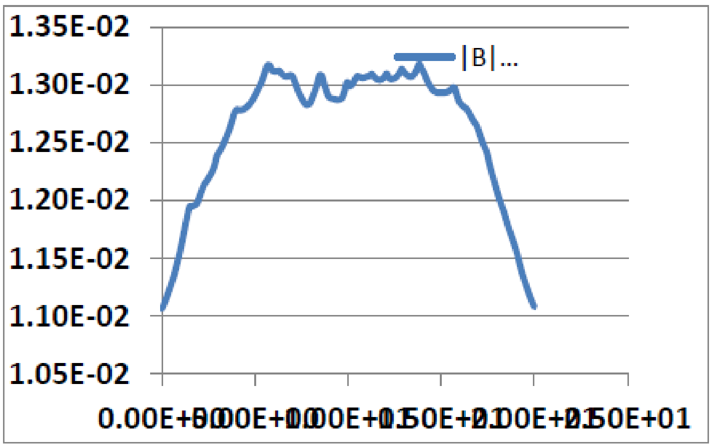

Fig. 3: Magnetic flux density B along the x-y contour.

Table 1: Magnetic flux density along x-y contour with 20mm length.

Length, mm	|B|, Tesla
0.00E+00	1.11E-02
1.43E+00	1.19E-02
2.86E+00	1.23E-02
4.29E+00	1.28E-02
5.71E+00	1.32E-02
7.14E+00	1.30E-02
8.57E+00	1.31E-02
1.00E+01	1.30E-02
1.14E+01	1.31E-02
1.29E+01	1.31E-02
1.43E+01	1.30E-02
1.57E+01	1.30E-02
1.71E+01	1.25E-02
1.86E+01	1.18E-02
2.00E+01	1.11E-02

As shown in figure 3, the magnetic flux density keeps convergent values starting from the distance 4.29 mm till 15.7mm. This is clearer in Table 1.

So if a PCB is aligned along the x-y contour, all of the copper traces which exist in the range of 4.39 mm – 15.7 mm will be induced synchronously. Hence we cannot dedicate this type of induction to a single copper trace.

The main challenge is how to drive the magnetic field, to limit its impact on a small range of distance up to 10 mil which is the standard width of copper trace (Johan *et al*, 2006) and to also achieve greater magnetic density.

To drive the magnetic lines, the core was extended since it has a larger relative permittivity. Hence, the core will not be limited between the two windings, it will arise out to involve as much as possible of the magnetic lines and to drive it to a predefined location. Through this method, the magnetic lines will prefer the pure iron (μ_x=14782) path than the air (μ_x=1). The new design is shown in Figure 4. The new design has 1000 turns using 36 AWD copper wire with 0.127mm diameter and electric conductivity σ = 58Ms/m. The coil is connected to 1 Ampere current source. Voltage drop inside windings can be evaluated by the following equation (John, 2006):

$$VD = (2 \times R \times I \times L) / CM \qquad (7)$$

where *VD* = Volts (voltage drop of the circuit), R = 12.9 Ohms/Copper or 21.2 Ohms/Aluminium (resistance constants for a conductor that is 1 circular mil in diameter and 1 foot long at an operating temperature of 75O C.), *I* = Amps (load at 100 turns), *L* = Feet (length of circuit from load to power supply), *CM*=Circular-Mils (conductor wire size). After Substituting all the variables *VD* = 132.455 Volts.

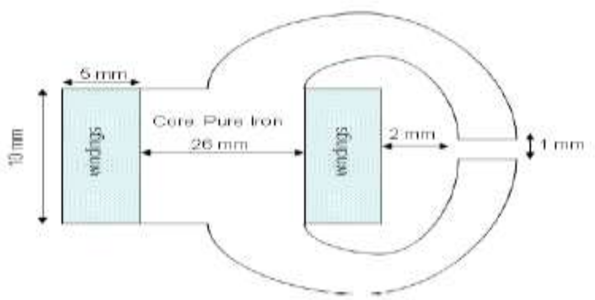

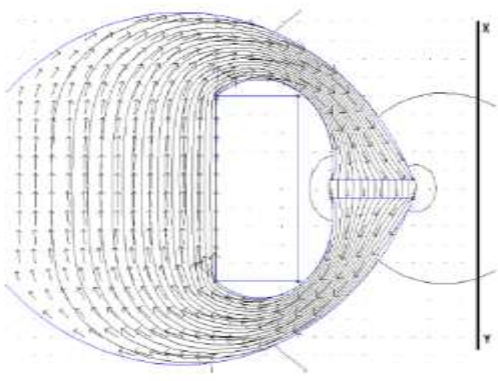

The resistance of the coil = 132.455 Ohm, so the power drop in the coil is calculated to be 132.455 Watts. The diameter of the core is increased to avoid magnetic line collisions which weaken flux density.

As shown in Figure 5, the iron core is the preferable path for magnetic lines. It is similar to light refraction. The lines start to get away from the core near the nozzle of core, so the magnetic density here is also concentrated near the nozzle.

Based on the previous equations (1-6), the magnitude of the flux density along the x-y contour can be evaluated which is 20 mm length and 5mm away from the nozzle. The following chart represents the flux density B along x-y:

Table 2: Magnetic flux density distribution for the new design along x-y contour.

Length, mm	|B|, Tesla
0.00E+00	1.16E-02
1.43E+00	1.26E-02
2.86E+00	1.35E-02
4.29E+00	1.48E-02
5.71E+00	1.64E-02
7.14E+00	1.79E-02
8.57E+00	1.92E-02
1.00E+01	1.98E-02
1.14E+01	1.90E-02
1.29E+01	1.80E-02
1.43E+01	1.65E-02
1.57E+01	1.49E-02
1.71E+01	1.36E-02
1.86E+01	1.25E-02
2.00E+01	1.17E-02

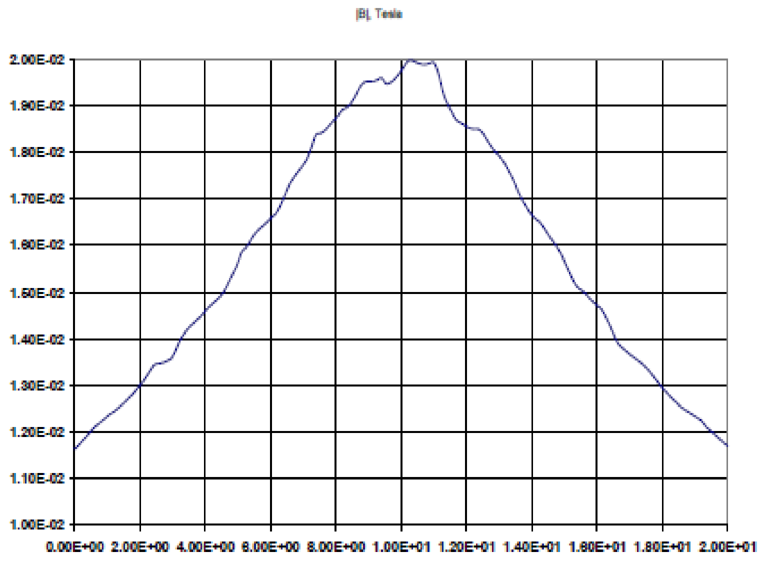

Fig. 6: Magnetic flux density B along the contour x-y aligned opposite to core nozzle

DISCUSSION

As shown in figure 6, the magnetic density concentrated in a narrow band distance which is between 8.57mm and 1.14mm is the segment directly opposite to core nozzle. Also by this design, the maximum value of flux density increased up to 1.98 x10^{-2} Tesla with difference 0.66 x 10^{-2} Tesla. Table 2 shows the distribution of flux density along the contour. The new mini coil features the ability to stimulate electromotive force in a narrow path (0.8-1.2) mm avoiding any considerable effect on the surrounding copper traces. The design of the new mini coil was carried out by Finite Element Method Magnetics simulation software. This paper shows the magnitude of flux density β along a parallel PCB.

CONCLUSION

The standard design for coils cannot be used to stimulate single copper traces inside PCB since it causes a wide band magnetic flux density so it will affect many traces synchronously. The new core design with a driving core will concentrate the field to a limited region so it can stimulate one copper trace avoiding any considerable induction on the surrounding traces. Also, this new design increases the flux density.

REFERENCES

Gisin, F. and Pantic-Tanner, Z. (2001) "Radiation from Printed Circuit Board Edge Structures", IEEE Transactions on Electromagnetic Compatibility, Vol. 37, No. 2.

Hadass, T., Shuki W., Alexander F., Eli P., Tamar P., Michal, L.,Alon, K., Yosef, Y., Izhar, B. (2011) " Mini-coil for magnetic stimulation in the behaving primate", "Journal of Neuroscience Methods", Vol.194. pp. 242–251.

Hockanson, D. M., Drewniak, J. L. , Hubing, T. H., Van Doren, T. P., Sha, F. Lam, C. and Rubin, L. (1997) "Quantifying EMI resulting from finite-impedance reference planes," IEEE Trans. Electromagn. Compat., vol. 39, no. 4, pp. 286–297.

Johan, M., Marion, W., Jean-Pau,l G., Elisabeth D. and Alain B. (2006) "High Current Densities In Copper Microcoils: Influence Of Substrate On Failure Mode", "Dtip Of Mems And Moems", pp.12-18.

John, B. and Stanislaw O. (2003) "Field line motion in classical electromagnetism", "Am. J. Physics", Vol.71, pp.220-221.

John T. C. (2009) "Copper Wire Tables", "National Bureau of Standards Handbook- Office of Engineering Standards Institute for Applied Technology National Bureau of Standards Washington".

Marco, L. (2005) "Radiated Susceptibility on the Printed-Circuit-Board Level: Simulation and Measurement", IEEE Transactions on Electromagnetic Compatibility, Vol. 47, No. 3.

Martin, S. (2011) "Avoid PC-Layout "Gotchas" in ISM-RF Products", "TUTORIAL 4636, Maxim Integrated Co.", pp.5-8.

Shaowei, D., Todd, H.H., and Daryl, G. B. (2008) "Using TEM Cell Measurements to Estimate the Maximum Radiation From PCBs With Cables Due to Magnetic Field Coupling" IEEE Transactions on Electromagnetic Compatibility, Vol. 50, No. 2, May 2008.

Shim, H. W. and Hubing, T. H. (2005) "Model for estimating radiated emissions from a printed circuit board with attached cables driven by voltage-driven sources," IEEE Trans. Electromagn. Compat., vol. 47, no. 4, pp. 899–907.

Young H.D. and Freedman R.A. (1998) " University Physics Textbook" 9th Edition pp. 943. Addison-Wesley Publishing Company, Inc.